Overhead Power cable Bragg signatures in Ka and Ku band high-resolution SAR imagery

Willetts, Ben; Stevens, Malcolm ; Stove, Andrew; Gashinova, Marina

Document Version
Peer reviewed version

Citation for published version (Harvard):
Willetts, B, Stevens, M, Stove, A & Gashinova, M 2017, Overhead Power cable Bragg signatures in Ka and Ku band high-resolution SAR imagery. in *Radar 2017: Radar 2017 International Conference on Radar System.* Institution of Engineering and Technology, 2017 International Conference on Radar Systems, Radar 2017, Belfast, United Kingdom, 23/10/17.

Overhead power cable Bragg signatures in K_a and K_u band high-resolution SAR imagery

B Willetts*, M B Stevens †, A G Stove*, M Gashinova*

**University of Birmingham, United Kingdom , {bxw942,stovea,marina.s.gashinova}@bham.ac.uk*
†Thales UK Ltd, United Kingdom, malcolm.stevens@uk.thalesgroup.com

Abstract

This paper presents spotlight SAR imagery and measurements that show specular and Bragg scattering from overhead power cables using two airborne high-resolution radar systems that operate in different frequency bands; the K_u (12-18 GHz) and K_a (26.5-40 GHz) band of frequencies. Previous cable measurements show that Bragg scattering occurs at K_a-band but did not measure Bragg scattering at 18 GHz whilst the measurements and imagery shown here demonstrate that Bragg lobes are measurable in K_u band as well as in K_a band. This paper also shows the advantage of having 50 mm resolutions in both the down range and cross range as this allows overhead cables to be easily distinguishable from the surrounding clutter. The ability to see a consistent set of Bragg locations along a given line for all cables is shown as well as the capability to estimate the same cable surface period with devices that operate at different frequencies.

1 Introduction

Overhead (OH) power cables have been the cause of aircraft accidents [1] and a method to enhance the detection of such obstructions is required to improve safety for aircraft flying at low-altitudes.

Several overhead power cable measurements have been made in the past [2, 3]. The previous measurements performed in the microwave bands have shown that most power cables behave as a smooth cylinder at 18 GHz and below [2] because the dimensions of the cable surface structure are small compared to the wavelength. The fact that only a single 'flash' is seen from the cables in this case suggests that in these circumstances real-beam radars will have difficulty in recognising overhead cables in cluttered scenes. At millimetre-wave (mmW) frequencies, however, additional peaks are seen in the angular response of such cables due to higher-order Bragg scattering modes being seen, caused by the periodic structure of the stranded cables. As noted in [2], these peaks occur at discrete angles (θ_n) (1) and are detectable out to an angle α away from broadside, which is determined by the range of angles for which surface normal angles are present on the stranded cable (2).

$$\theta_n = \sin^{-1}\left(\frac{n\lambda}{2L}\right) \qquad \text{where } n \text{ is an integer} \qquad (1)$$

$$|\alpha| = \tan^{-1}\left(\frac{\pi D}{P}\right) \qquad (2)$$

where λ is the wavelength of the incident planar EM wave, L is the cable surface period, D is the cable diameter and P is the helical pitch of the cable.

An important result reported in this paper is that we have seen grating lobes at K_u band, due to the different cable geometry of the cables we have observed as opposed to those described in [2]. This is made clear if we equate ϕ_n in (1), for the case n = 1, with α in (2) and make the small angle assumption that $\sin^{-1}(x) \approx \tan^{-1}(x)$ we can see that higher-order Bragg modes appear when

$$\lambda \leq \pi DL/P \qquad (3)$$

so the longest wavelength at which higher-order modes are seen depends on the cable geometry and they can occur at longer wavelengths with more modern cable geometries.

Research conducted at 150 GHz [4] showed the potential of getting additional, more closely spaced peaks which could be utilised to make a viable wire-detection system, but if an aircraft already carries a radar it would of course be desirable if its hardware could also provide an obstacle-avoidance function to avoid the need to mount a separate sensor onto the platform. This paper shows spotlight SAR imagery gained from radar systems that clearly show the power cables. The high range resolution of a system such as I-Master together with the use of the SAR processing techniques to give high cross-range resolution will help the detection of OH power cables against the clutter background. The available real-mode angular resolution of the system can also be exploited in geometries which are unsuitable for SAR.

Compared with a dedicated, real aperture, millimetre-wave radar, using SAR for this purpose requires much higher processing power to form the high resolution images, but since the SAR processing is already present in the radar, in this case using it for wire detection comes almost for free. Real-time processing of images with the same resolution as those presented can be performed for the I-Master system and is also attainable for the Bright Spark system. The slanted side-looking viewpoint required to gather SAR imagery can be used to supplement information from a simple forward-looking sensor or map information.

The second section briefly describes two different scenarios that contain different types of high voltage power cables together with single-look spotlight SAR images that were obtained from measuring these scenarios on board an aircraft. The angular profiles obtained from the previous high resolution images are shown in both graphical and tabular format as well as the estimated surface period obtained when using (1). The paper then concludes with the main findings and also a brief discussion on possible future work.

2 Spotlight SAR Images

Two different scenarios were measured using high resolution spotlight SAR techniques with the Bright Spark and I-Master radar systems developed at Thales UK. The Bright Spark radar is based on the K_u-band I-Master system discussed in [5] although Bright Spark operates in the K_a band with a pixel resolution of around 50 mm. The results presented were collected on a small aircraft, a Cessna 406, to gain spotlight images of two different types of OH cables. The first scenario, Scenario 1, contained three separate lines of 3-phase power cables. An optical image of Scenario 1 is shown in Fig 1.

Fig 2 shows a multi-look SAR image of Scenario 1 obtain using the Bright Spark device (K_a band). The three transmission lines are labelled 'A,' 'B' and 'C.' 'A' is above (to the North of) the farm, and is probably a relatively-low voltage line and seems to supply power to the farm. 'B' is probably a 33kV 'grid' line which is in the region and 'C' is probably another lower-voltage lines. The sections labelled '1,' '2' and '3', and '4' for line 'B' only are separate sections of line between different support poles. The wires are straight, in the horizontal plane, between the poles but their direction can change at the poles. Each section consists of three parallel wires, carrying the three separate phases.

The second scenario, Scenario 2, consisted of a single set of nine cables suspended between two large pylons. Scenario 2 is labelled as a 275/400 kV distribution line in Fig 3 and an optical picture of this scene is shown in Fig 4.

The single-look spotlight SAR images gained from Scenario 1 for three different aspect angles are visible in Fig 5 using the I-Master (K_u band) system and in Fig 6 by the Bright Spark system (K_a band). Figure 7 displays single-look spotlight SAR images gained from Scenario 2 for three different aspect angles. Figs 5-7 show the specular scattering region, a null period where the cables are not detectable and then the first-order Bragg scattering region. As would be expected, when the cables are images at normal incidence a strong return is seen, (Figs 5a, 6a and 7a). At more oblique angles (Figs 5b, 6b and 7b) the strong return is no longer seen but when the cables are images from the direction of the first Bragg mode (Figs 5c, 6c and 7c) the strong returns reappear.

Since Fig 5 was obtained using a K_u band device it can be seen that a higher-order Bragg scattering region exists which has not been observed in the earlier work. Following equations (1) and (2) we can therefore assume that the geometry is such that $|\alpha| > \theta_1$. Additionally, Fig 8 shows how detailed the Scenario 1 cables appear in the high resolution spotlight SAR image obtain by the K_a-band Bright Spark system for both the specular and Bragg scattering regions.

Figure 1: Optical image obtained from Google Maps that shows an aerial view of Scenario 1.

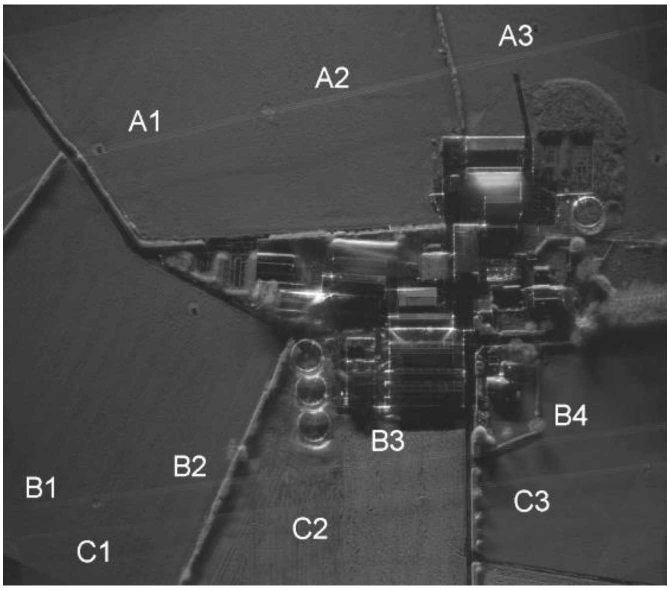

Figure 2: Labelled multi-look spotlight SAR image of the farm scenario that consists of three spans of OH power cable

Figure 3: Map showing location of scenario 2 [7].


Figure 4: Optical image obtained from Google Maps that shows an aerial view of Scenario 2.

3 Angular Profiles

The angular variations in the scattering strength can be deduced by performing an inversion of the SAR image formation process. Figures 9 and 10 show the results obtained for different Bragg modes from Scenario 1 at K_u band and K_a band respectively. The upper graph in each figure shows the response as a function of angle so the directions of the different Bragg modes can be seen, whilst the three enlargements below show the detail from each cable. The sharp peaks seen in Figures 9 and 10 support the view that the scattering behaviour is explained by the simple Bragg scattering model.

Table 1 shows the Bragg lobe positions measured for Scenario 1. The standard deviation was calculated from the difference in the spacing between the two first order Bragg modes and the zeroth order mode and between the three wires in each section of each line. The very high consistency shows that the mean direction in which the lobes are seen can be determined to an accuracy much greater than the width of the reconstructed lobes (lower parts of Figs. 9 and 10).

The angles of the Bragg scattering are very consistent between the wires in the different sections of each line, which is an indication of the reliability of the measurements. The direction of the scattering varies slightly between the lines, suggesting that each is made from a slightly different type of cable from the others, although this variation is small, suggesting that the different cables have a very similar style of construction, The scattering angle at K_u band is also not exactly twice that at K_a band although the centre frequencies of the two systems in this scenario differed by approximately a factor of two.

Table 2 shows the estimated surface period for each line at K_a band and K_u band, derived from inverting (1). As expected, the values are highly consistent for each line. Although the type of cables used in these lines has not been identified, the values of the surface period are similar to those reported in [4] and are thus plausible. It should be noted that they are significantly greater than those of the cables measured in [2] which would explain why higher-order lobes are seen at K_u band with these cables.

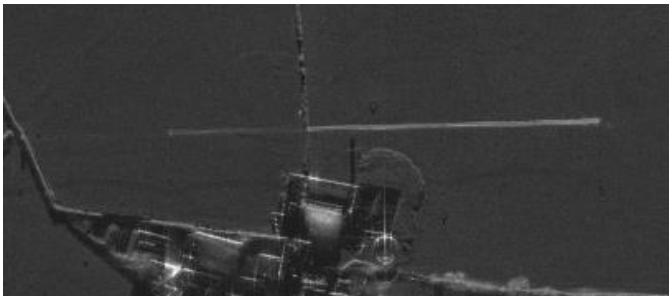
a)

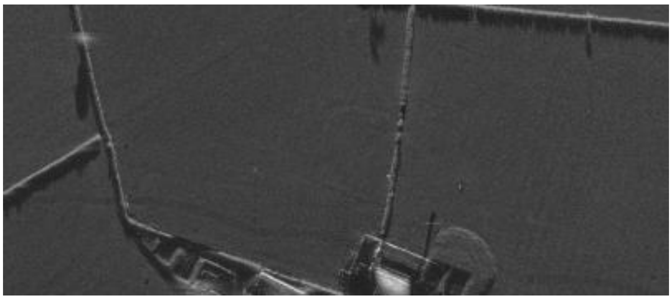
b)

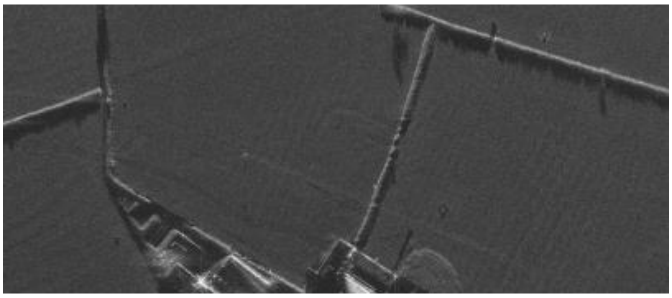
c)

Figure 5: I-Master single-look Spotlight SAR images obtained from measuring Scenario 1 whilst on-board a fixed-wing aircraft. a) Specular reflection, b) first null measured off-specular, c) first off-specular peak.

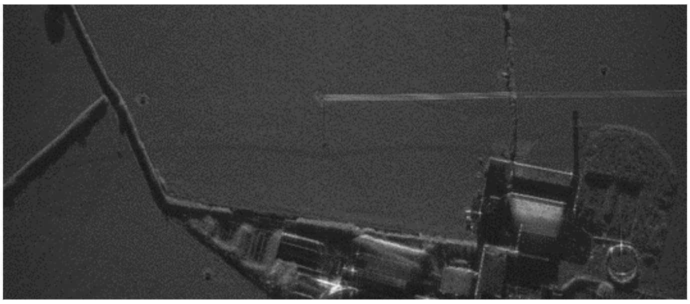

a)

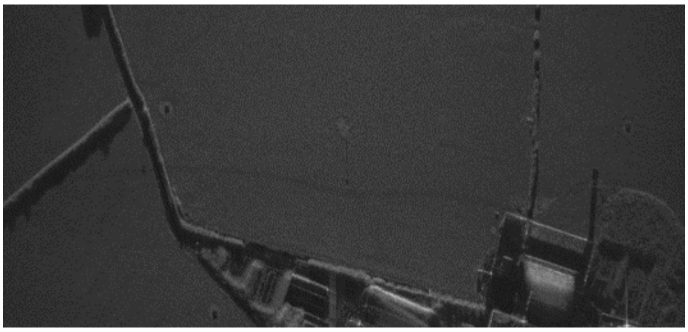

b)

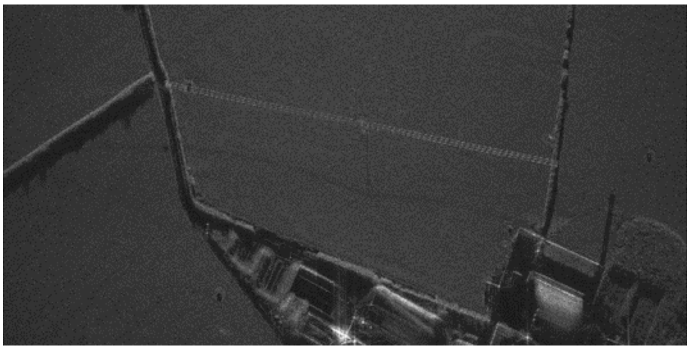

c)

Figure 6: Bright Spark single-look Spotlight SAR images obtained from measuring Scenario 1 whilst on-board a fixed-wing aircraft. a) Specular reflection, b) first null measured off-specular, c) first off-specular peak.

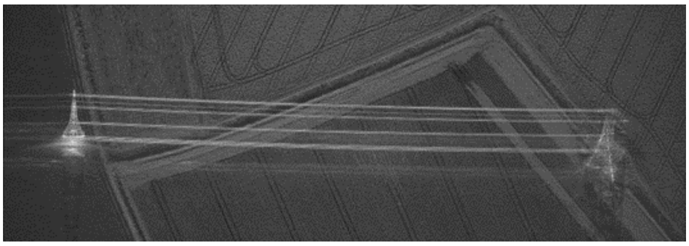

a)

b)

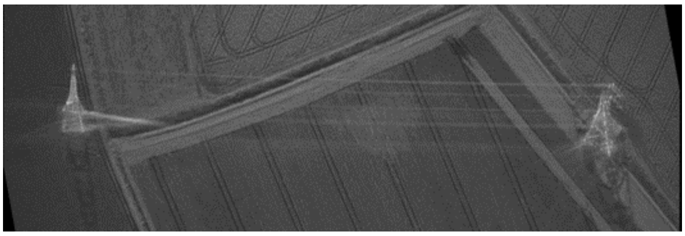

c)

Figure 7: Bright Spark single-look Spotlight SAR images obtained from measuring Scenario 2 whilst on-board a fixed-wing aircraft. a) Specular reflection, b) first null measured off-specular, c) first off-specular peak.

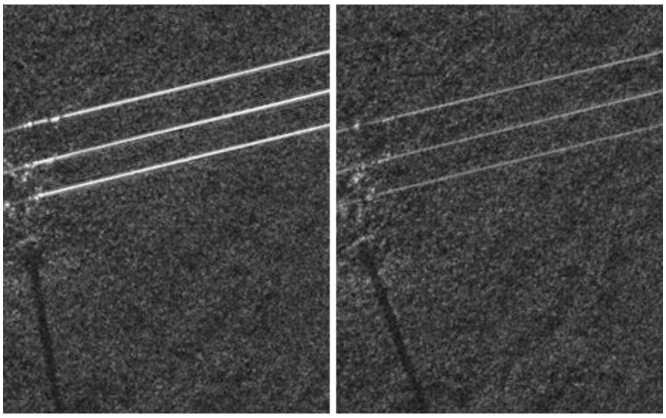

Figure 8: Close-up image of cable taken from the processed high resolution spotlight SAR images for the specular scattering region (left) and the Bragg scattering region (right) in Scenario 1 (Figs 6a and 6c).

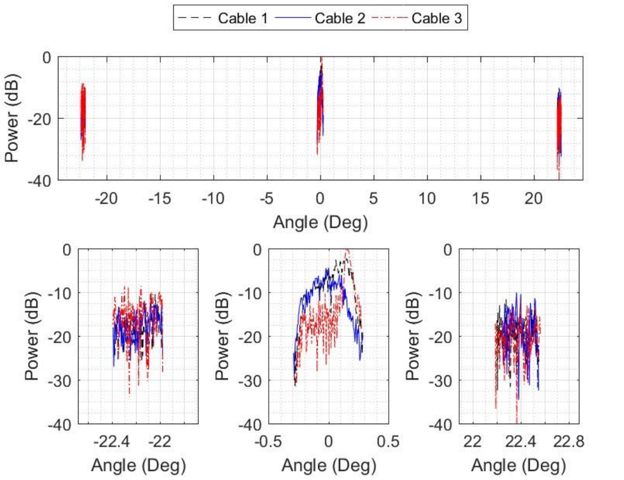

Figure 9: K_u band (12-18 GHz) angular return from the three cables at section A2.

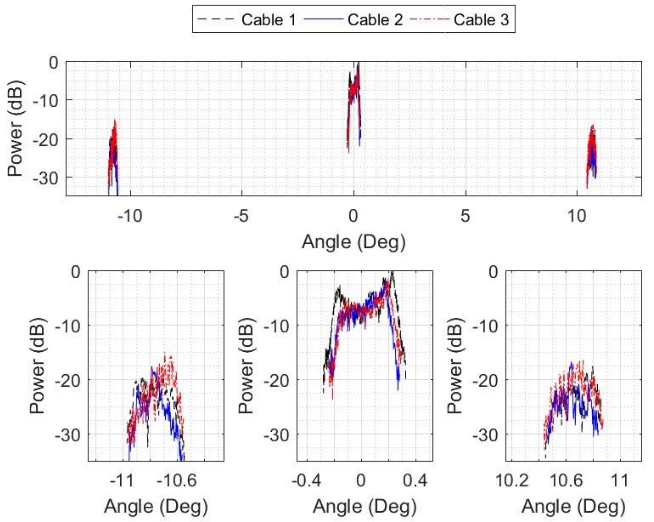

Figure 10: K_a band (26.5-40 GHz) angular return from the three cables at section A3.

Line/ Span	1	2	3	4
A	Ka: 10.5±0.05°	Ka: 10.8±0.02°	Ka: 10.7±0.02°	
	Ku: 22.9±0.006°	Ku: 22.4±0.02°	Ku: 22.5±0.07°	
B	Ka: 9.3±0.01°	Ka: 9.1±0.01°	Ka: 8.9±0.002°	Ka: 9.5±0.01°
			Ku: 19±0.01°	
C	Ka: 12.4±0.01°	Ka: 12.2±0.01°	Ka: 12.6±0.05°	

Table 1: Measured Bragg peak locations fitted to a Gaussian distribution [μ (mean) ± σ (standard deviation)].

Line/Span	Mean Surface Period (L) [K_u band]	Mean Surface Period (L) [K_a band]
A	24 mm	24 mm
B	28 mm	27 mm
C		20 mm

Table 2: Estimated cable surface period using (1) for each line at both K_a and K_u band.

4 Conclusion

The results presented show that Bragg scattering from overhead power cables are detectable down to K_u band. The Bragg scattering observed was consistent for a given distribution line for each cable in the three phase line. The estimated surface period of the cable, which can be used for cable classification, was also consistent at K_a-band and K_u band whilst giving a reasonable value in the order of centimetres.

Acknowledgements

This work was funded by Thales and EPSRC. Development of the I-Master radar was part funded by the UK MoD and Bright Spark was developed with funding from Dstl UK. This paper also contains OS data © Crown copyright and database right (2017).

References

[1] Air Accidents Investigation Branch, “AAIB Bulletin 10/2009”, October 2009.

[2] H. Al- Khatib, "Laser and millimeter-wave backscatter of transmission cables,” Proc. SPIE 0300, p.212, 1981.

[3] K. Sarabandi, L. Pierce, O. Yisok and F. T. Ulaby, "Power line: radar measurement and detection algorithm for polarimetric SAR images," IEEE Trans. Aerosp. Electron. Syst., Vol. 30, No.2, pp.63-2643, 1994.

[4] B. Willetts, "Low-THz overhead power cable signatures: The effect of surface features on Low-THz reflectivities," 2016 17th International Radar Symposium (IRS), Krakow, pp. 1-6, 2016.

[5] M. B. Stevens and D. L. Perks, "I-Master RADAR: Recent trials results," IET International Conference on Radar Systems (Radar 2012), Glasgow, UK, 2012, pp. 1-5.

[6] "Eastern Power Networks PLC Distribution Area, 400kV, 275kV, 132kV and 33kV systems" in UK Power Networks, 2013.

[7] " TF - National Grid high-voltage cable location," in National Grid, 2017. Accessed: Feb. 16, 2017.